



Minerva Access is the Institutional Repository of The University of Melbourne

**Author/s:**

Connolly, AR;Hirani, R;Ellis, AV;Trau, M

**Title:**

A DNA Circuit for IsomiR Detection

**Date:**

2016-11-17

**Citation:**

Connolly, A. R., Hirani, R., Ellis, A. V. & Trau, M. (2016). A DNA Circuit for IsomiR Detection. *Chembiochem*, 17 (22), pp.2172-2178. <https://doi.org/10.1002/cbic.201600452>.

**Persistent Link:**

<https://hdl.handle.net/11343/291845>

## Author Manuscript

**Title:** A DNA Circuit for IsomiR Detection

**Authors:** Ashley Rex Connolly, PhD; Rena Hirani, PhD; Amanda V Ellis, PhD; Matt Trau, PhD

This is the author manuscript accepted for publication and has undergone full peer review but has not been through the copyediting, typesetting, pagination and proofreading process, which may lead to differences between this version and the Version of Record.

**To be cited as:** ChemBioChem 10.1002/cbic.201600452

**Link to VoR:** <http://dx.doi.org/10.1002/cbic.201600452>

# A DNA Circuit for IsomiR Detection

Ashley R. Connolly<sup>#\*</sup>, Rena Hirani<sup>‡</sup>, Amanda V Ellis<sup>#</sup> and Matt Trau<sup>†\*</sup>

**Abstract:** A synthetic DNA oligonucleotide has been programmed to function as a biological circuit to detect 5' IsomiRs. The circuit comprises of two integrated DNA switches. The first is 'activated' when a DNA probe is enzymatically modified by a reverse transcriptase that incorporates nucleotides complementary to the 5' region of a micro RNA (miRNA). Addition of the correct number and sequence of nucleotides enables the probe to assemble into an asymmetric DNA hairpin. The reconfigured hairpin probe then primes an internal polymerisation reaction resulting in the synthesis of a symmetrical DNA hairpin. This activates the second switch which then initiates the amplification of reverse transcribed miRNA through a continuous cycle of DNA nicking and polymerisation. The DNA circuit enables sensitive and rapid detection of femtomoles of a miRNA transcript under isothermal conditions.

## Introduction

Micro-RNAs (miRNAs) are short sequences of non-coding RNA capable of modulating gene expression. This occurs by hybridisation of the miRNA to a specific messenger RNA (mRNA) transcript. As a result, dysregulated miRNAs can serve as diagnostic or prognostic biomarkers of pathogenic infections, genetic disease and cancer [1]. miRNAs are often annotated as a single sequence, although many length and nucleotide variants of the same miRNA have been identified [2]. These variants named, isomiRs, have been shown to have distinct biological functions, which are often defined by nucleotides at the 5' end of the miRNA [3].

The biological significance of miRNAs has stimulated the development of techniques using a thermally stable polymerase to replicate reverse transcribed miRNA by thermal cycling [4]. However, amplification of miRNAs at constant temperature (isothermal) has emerged as a more attractive alternative as it is rapid and does not require specialized instrumentation [5].

Numerous isothermal miRNAs amplification methods have been developed that utilise the hybridisation chain reaction [6], DNAzymes and enzymes [7] which enable miRNAs to be measured with high sensitivity when coupled to electrochemical, fluorescent or enzymatic detection systems [5, 8]. However,

analysis often proceeds with an accuracy defined by the specificity of miRNA hybridisation to its complementary DNA counterpart [1a, 1b, 9]. This can often confound analysis because length and sequence variations of the isomiRs are often difficult to distinguish by hybridisation. Therefore, advances in the analysis of the 5' region of a miRNA will help to refine miRNA function in research laboratories and classify disease in diagnostic laboratories.

Herein we report a new isothermal process to accurately detect miRNAs with an emphasis on identifying 5' length and sequence variations. The process was inspired by elegantly designed DNA switches that respond to biological triggers [10]. We devised a functional DNA circuit composed of two integrated switches that enable amplification and high fidelity detection of miRNA. The entire detection and amplification process is accomplished using a synthetic 'switching nucleic acid probe' (SNAP) composed of multiple distinct DNA modules. miRNA induced activation of the biological circuit has been characterized using gel electrophoresis and real time detection and amplification of trace amounts of a synthetic miRNA in a purified RNA extract is demonstrated. The biological circuit enables femtomoles of a miRNA transcript to be detected in less than 15 min, showing great promise for biomedical research and clinical diagnosis.

## Results and Discussion

A DNA switch designed to enable the biological circuit to be selectively 'activated' by a specific 22nt miRNA is depicted in Scheme 1A. The hybridisation module in the SNAP is designed to engage a specific miRNA (Scheme 1A, I). A reverse transcriptase (M-MuLV) incorporates a specific sequence of nucleotides into the 3' region of the probe (Scheme 1A, II). This sequence is defined by the miRNA and the circuit is 'activated' only if the correct nucleotide sequence is incorporated. The SNAP also contains an internal 'switching module' (Table 1) that complements the nucleotides incorporated into the 3' region of the probe. This enables the activated probe to be 'reconfigured', which is induced by the free energy of base pair formation. This reconfiguration is induced by the proximity of the switching module to the newly incorporated nucleotides and results in an asymmetric DNA hairpin (Scheme 1A, III). Incorporating an incorrect nucleotide sequence during activation retards reconfiguration and limits amplification. This design feature promotes miRNA 'proof reading', which enables the circuit to be selectively 'activated' so a unique 5' isomiR can be detected.

The second switch in the biological circuit is designed to initiate DNA amplification to enable signal transduction. This is achieved in a subsequent reaction using a DNA nicking endonuclease and DNA polymerase to replicate multiple copies of the reverse transcribed miRNA in a non-linear cyclic chain reaction [7a, 11]. The amplification procedure, depicted in Scheme 1B, is only initiated when the SNAP has been

[#] Dr. A.R. Connolly  
Flinders Centre for Nanoscale Science and Technology  
Flinders University  
Sturt Road Bedford Park SA, 5042, Australia

[‡] Dr. R. Hirani  
Australian Red Cross Blood Service  
Sydney, NSW, Australia  
rhirani@redcrossblood.org.au

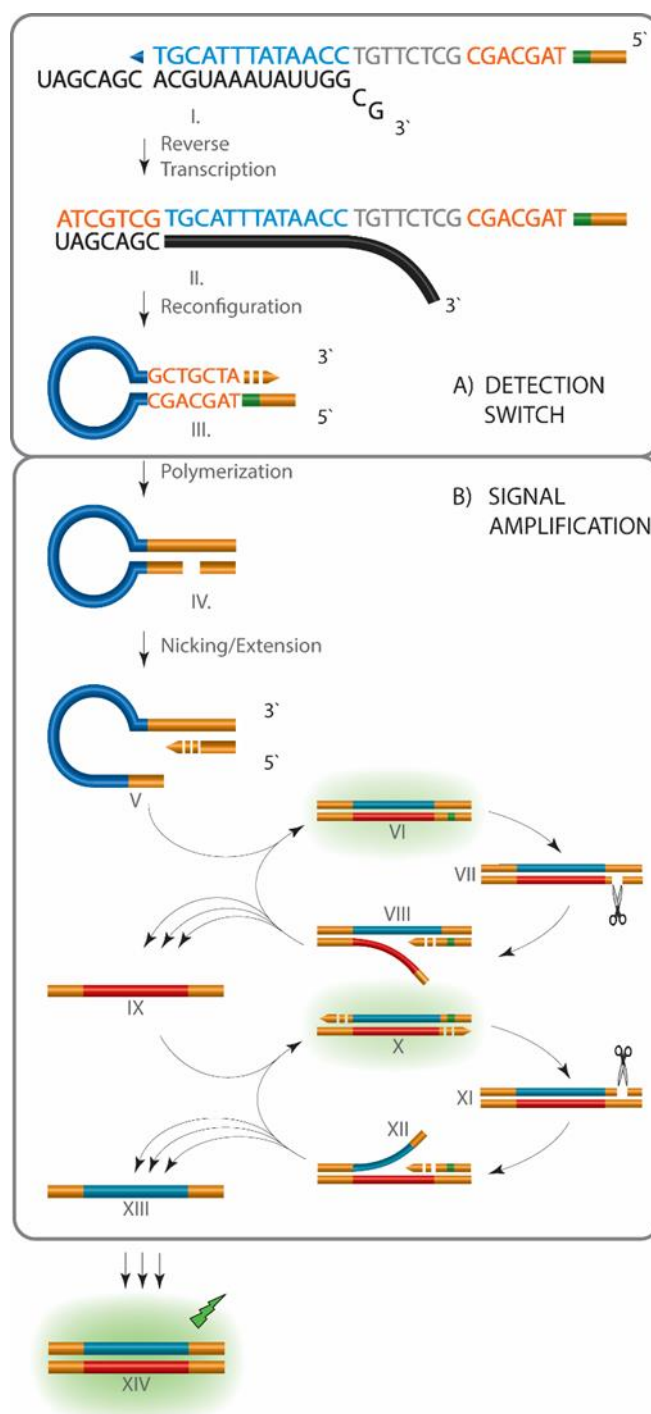
[#] Professor, A.V., Ellis  
Flinders Centre for Nanoscale Science and Technology  
Flinders University  
Sturt Road Bedford Park SA, 5042, Australia

[†] Professor M. Trau  
Australian Institute for Bioengineering and Nanotechnology.  
The University of Queensland  
Brisbane, QLD, 4072, Australia.

successfully reconfigured into an asymmetric DNA hairpin (Scheme 1A, III). The 3' region of the hairpin primes an internal polymerisation reaction resulting in the production of a symmetric DNA hairpin (Scheme 1B, IV). A dormant endonuclease recognition domain in the 5' region of the probe is also activated with the formation of the symmetric DNA hairpin. This provides a suitable substrate for endonuclease nicking, which 'switches on' the amplification and signal transduction process. Polymerisation is initiated from the 3' end of the nicked DNA (Scheme 1B, V). Polymerisation also reconfigures the hairpin into duplex DNA (Scheme 1B, VI) as the endonuclease nicking domain is regenerated. A subsequent cycle of nicking (Scheme 1B, VII) and polymerisation (Scheme 1B, VIII) displaces a copy of the reverse transcribed miRNA (Scheme 1B, IX) during re-synthesis of duplex DNA (Scheme 1B, VI). With each synthesis cycle the DNA duplex is regenerated and the replicated DNA (Scheme 1B, IX) engages a subsequent probe to initiate an additional cycle of polymerisation (Scheme 1B, X), nicking (Scheme 1B, XI) and displacement (Scheme 1B, XII) to rapidly amplify a copy of the reverse transcribed miRNA (Scheme 1B, XIII). Once initiated, these reactions cycle continuously in a single tube at uniform temperature to rapidly produce complementary DNA products (Scheme 1B, IX and XIII) that combine to form a DNA duplex (Scheme 1B, XIV) at a rate suitable for optical detection using a DNA intercalating fluorescent dye.

The sequence of the SNAP is shown in Table 1. The probe contains a 13 nucleotide hybridisation module designed to engage a specific miRNA transcript, to enable 7 nucleotides to be incorporated into the 3' region of the probe.

A key component to activating the detection switch involves generating single stranded DNA to enable the incorporated nucleotides to interact with the switching module. This reconfiguration can occur by utilising a reverse transcriptase with a functional RNase H domain [12]. This ensured a small amount of miRNA was hydrolysed, which enabled the circuit to be activated. More comprehensive hydrolysis of the miRNA was achieved by introducing RNases into the reaction to promote reconfiguration of the probe, but this also appeared to compromise the efficiency of amplification (Supplementary Figure S1). Nevertheless, both approaches proved sufficient to promote the reconfiguration required to activate the detection switch.



**Scheme 1.** SNAP detection of miRNA. A miRNA (black) induces enzymatic modification to the hybridisation module of the probe (blue) during reverse transcription (Scheme 1A). The probe also contains a switching module (orange) that complements the incorporated nucleotides, to enable reconfiguration into asymmetric hairpin. Reconfiguration primes an internal polymerisation reaction (Scheme 1B) that activates an endonuclease nicking domain (green). This initiates a continuous series of nicking and displacement reactions that produce DNA at amounts sufficient for optical detection.

The different transition states of the SNAP (Scheme 1A) in an experimental system were analysed by identifying the reaction intermediates using gel electrophoresis. Figure 1 shows the miRNA target and probe have a high mobility through the gel (Figure 1, lane 1 and 2). The addition of 7 nucleotides to the probe during reverse transcription (Scheme 1A, II) is evident by the reduced mobility of the RNA:DNA heteroduplex (Figure 1, lane 4). Following hydrolysis of the miRNA, the activated probe forms an asymmetric DNA hairpin (Scheme 1A, III) (Figure 1, lane 5) that has the same electrophoretic mobility as a synthetic reproduction of the asymmetric DNA hairpin. It is clear that miRNA detection is dependent on enzymatic 'activation' of the SNAP, since no nucleotide incorporation and SNAP reconfiguration was detectable when reverse transcriptase was omitted from the reaction (Figure 1, lane 3).

**Table 1.** Oligonucleotide Sequences. (1) The synthetic DNA Probe contained a RNA hybridisation module (blue), a switching module (orange) and Nt.BstNBI restriction site (green). The probe contained 8 arbitrary nucleotides (grey) to ensure reconfiguration produced a thermodynamically stable asymmetric DNA hairpin with a 21 nucleotide loop, (2) the synthetic miRNA sequence and (3) sequence of a mutated SNAP containing 3 nucleotide mismatches (underlined) in the switching module.

		Sequence (5'-3')
(1)	Probe	ATCCACGGGCACTGCGAGTCTTAGCAGCGCTCTT GTCCAATATTTACGT
(2)	miRNA Target	UAGCAGCAGGUAAAUAUUGGCG
(3)	Mutated Probe	ATCCACGGGCACTGCGAGTCAATGCGAGCGCTCTT GTCCAATATTTACGT

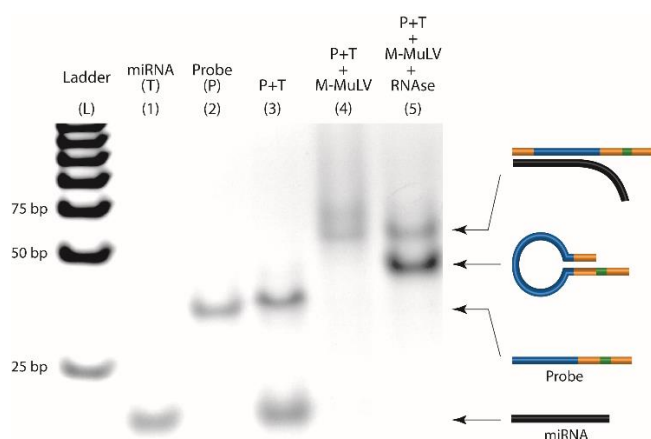


**Figure 1.** The transition states of the SNAP. The reagents and transitional states of the SNAP are indicated right of the image. The mobility of the synthetic miRNA target (lane 1) and the probe (lane 2) remained unchanged when mixed together (lane 3) but decreased with the addition of reverse transcriptase (M-MuLV) to the reaction (lane 4). RNase degradation of the miRNA enabled the formation of an asymmetric DNA hairpin loop (lane 5), which had the same electrophoretic mobility as that of a synthetic reproduction of the asymmetric DNA hairpin (data not shown).

SNAP amplification outlined in Scheme 1B, functions by replicating multiple DNA copies of the miRNA in a cyclic polymerisation reaction. This is achieved by implementing nicking and polymerisation reactions that work in concert to non-linearly produce double stranded (ds) DNA copies of the miRNA. Amplification is initiated by the conformationally active asymmetric DNA hairpin (Scheme 1A, III), which in the current application is characterised by a 21 nucleotide loop stabilised by a 7 nucleotide stem. The 3' recessed stem primes polymerisation of 21 nucleotides to form a symmetrical DNA hairpin (Scheme 1B, IV). This process also activates a dormant Nt.BstNBI endonuclease DNA nicking domain. This domain was positioned to ensure the resultant 24 base pair (bp) DNA duplex maintained sufficient thermal stability to prime a polymerisation reaction. At 55 °C the nicking and polymerisation reactions cycle continuously to rapidly produce multiple 29 bp dsDNA copies of the miRNA (Scheme 1B, XIV) from the 53 bp DNA duplexes (Scheme, 1B, VI and X).

The products produced by SNAP amplification of reverse transcribed miRNA are depicted in Figure 2. In the absence of DNA polymerase a product with a mobility consistent with the asymmetric hairpin loop (Scheme 1A, III) was identified by gel electrophoresis (Figure 2, lane 1). In the absence of the DNA nicking endonuclease a product with a mobility consistent with the symmetrical hairpin loop (Scheme 1B, IV) was observed in an experimental amplification system (Figure 2, lane 2). Amplification initiated with nicking endonuclease and DNA polymerase produced a product with mobility consistent with the 53 bp DNA duplexes (Scheme 1B, VI & X) Figure 2 (lane 3). Amplification also produced dsDNA copies of the reverse transcribed miRNA (Scheme 1B, XIV), which can be seen in the same reaction as a more mobile 29 bp reaction product (Figure 2, lane 3).

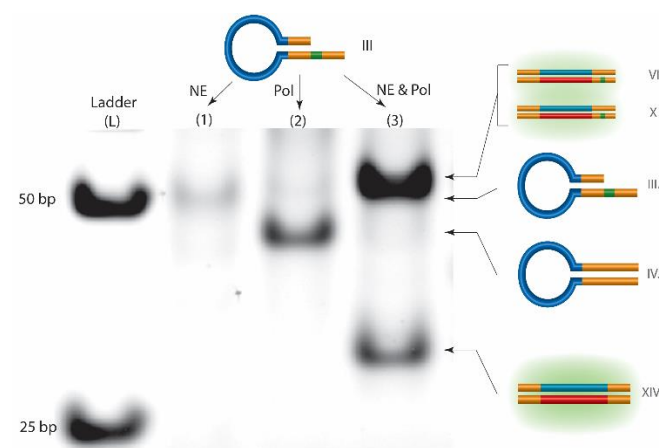


**Figure 2.** SNAP Amplification: The synthetic miRNA was added to a reverse transcription reaction to generate 'activated' probe (Scheme 1A, III). Replicate reactions containing the 'activated' probe were prepared and incubated with 1) Nt.BstNBI nicking endonuclease, 2) Bst large fragment DNA polymerase and 3) both enzymes for 1 hour at 37 °C. The reaction products were analysed by non-denaturing PAGE. The transitional states relating to Scheme 1 and reaction products are depicted adjacent to the image

The progress of the SNAP amplification reaction was also characterised in real time (Figure 3) by monitoring the fluorescence produced when Syto 9 intercalated into the duplex DNA reaction products (Scheme 1B, VI, X & XIV). It is clear that amplification is dependent on the DNA polymerase since there was no amplification when it was omitted from the reaction (Figure 3A). The DNA nicking enzyme is also an essential component for a functional circuit since there was no amplification in its absence (Figure 3B). Within minutes of initiating the reaction with both the nicking enzyme and DNA polymerase there was a large increase in fluorescent signal, which was attributed to the formation of DNA amplification products (Figure 3C). After 5 min the signal increased by approximately 3.3 fold. During the early stages of amplification the signal increased at approximately 3.2 fluorescent units per min, which decreased to 1 unit per min as the reaction progressed. This reduction in amplification with time was attributed to the consumption of the SNAP, which is an essential component for non-linear amplification. The reaction yield increased with the introduction of additional probe into either the reverse transcription or amplification reaction (Supplementary Figures S2 and S3). The rate of amplification also increased by adding additional nicking endonuclease and DNA polymerase (Supplementary Figure S4 and S5).

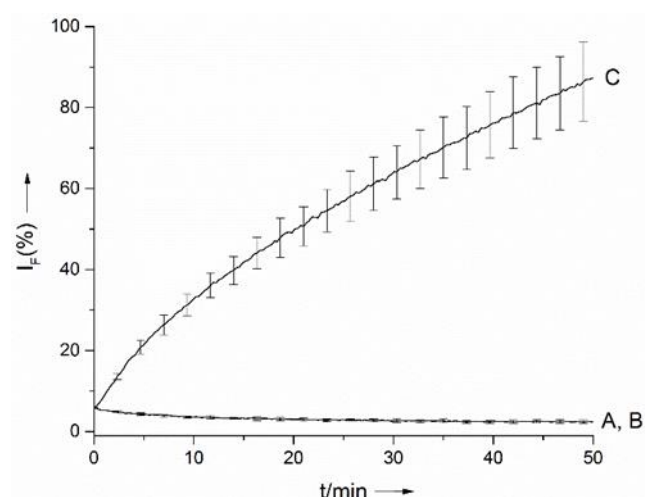


**Figure 3.** SNAP amplification: 859 fmol of synthetic miRNA was added to a reverse transcription reaction to generate 'activated' probes (Scheme 1A, III). Replicate reactions containing the 'activated' probes were prepared and incubated with a dye (Syto 9) that fluoresces when intercalated into DNA. The fluorescence emission was monitored following A) the addition of Nt.BstNBI endonuclease, B) Bst large fragment DNA polymerase and C) both enzymes. Values represent the fluorescence mean  $\pm$  standard deviation of quadruplicate reactions at the indicated time

Variability in the sequence of nucleotides in the 5' region of a miRNAs (5' isomiRs) can influence biological function [13] and confound miRNA analysis [14]. The 5' region of a miRNA also defines the nucleotides incorporated into the 3' region of the SNAP during reverse transcription. Incorporation of nucleotides that complement the SNAP switching module will promote probe

reconfiguration, while 5' isomiRs or mutations in the switching module, may limit amplification and detection. Therefore, the fidelity of 5' isomiR detection was investigated using a SNAP with a mutated switching module.

A reaction initiated with a SNAP containing no mutations produced the expected 53 bp (Scheme 1B, VI & X) and 29 bp (Scheme 1B, XIV) DNA reaction products (Figure 4, lane 1). Interestingly, a mutated SNAP, which harbored 2 nucleotide mutations within the 7 nucleotide switching module (Table 1) produced a small amount of two DNA products (Figure 4 lane 2). One had a mobility consistent with an asymmetric hairpin loop (Scheme 1A, III), which is expected to be a 21nt loop stabilised by a 5 base pair DNA stem. A small amount of a second DNA product had a mobility consistent with the more mobile 29 bp product produced by numerous cycles of DNA amplification (Scheme 1B, XIV). This suggests the mutated probe retained the capacity to be activated, but the level of DNA amplification was substantially reduced. In the absence of miRNA, only DNA consistent with the 49 nucleotide ssDNA SNAP was detected (Figure 4, lane 3).

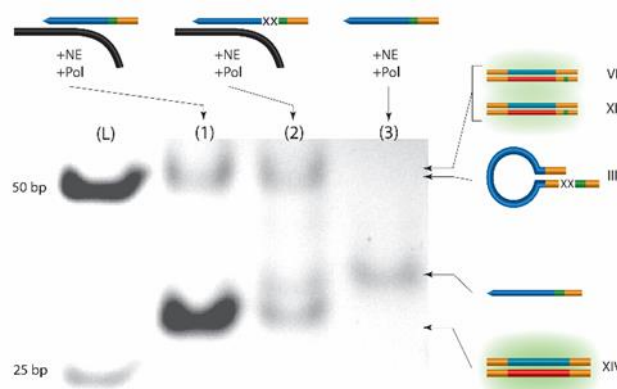


**Figure 4.** Fidelity of the switching module: Replicate reverse transcription reactions contained miRNA and 1) a SNAP with a switching module complementary to the 5' miRNA sequence, 2) a SNAP with 2 nucleotide mutations in the switching module (Table 1) and 3) no miRNA. Residual RNA was hydrolysed and the products were amplified using Bst DNA polymerase and Nt.BstNBI endonuclease. The reaction products were analysed by non-denaturing PAGE. The transitional states relating to Scheme 1 and reaction products are depicted adjacent to the image.

The impact of the mutated switching module was clearly evident when the reaction was monitored in real time. After 15 min there was no significant statistical change in fluorescence when the reaction was initiated with the mutated SNAP (Figure 5A). This was attributed to the inability of the 'activated' probe to prime an internal polymerisation reaction, despite folding into the appropriate hairpin configuration (Scheme 1A, III). As a result, the average rate of amplification for the duration of the reaction was 7.7 fold lower than that measured in an identical reaction that contained a SNAP harboring no mutations (Figure 5B). This demonstrates the specificity of the biological circuit and the stringency of the nucleotide sequence required to initiate DNA

amplification. Despite the high activation fidelity, a 1.8 fold increase in fluorescence was measured in the reaction initiated with the mutated probe (Figure 5A). This mode of amplification was statistically significantly different from the level of background amplification measured when miRNA was omitted from the reaction (Figure 5C) and may be attributed to the fidelity of the reverse transcriptase and DNA polymerase [15].

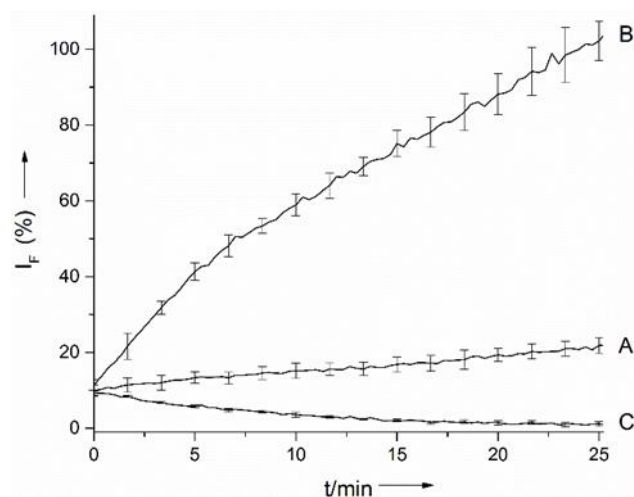


**Figure 5.** Fidelity of the switching module: Replicate reverse transcription reactions contained 1.7 pmol of miRNA and A) a SNAP with 2 nucleotide mutations in the switching module, B) a SNAP with no mutations in the switching module and C) no miRNA. Residual RNA was hydrolysed and the products were amplified using Bst DNA polymerase and Nt.BstNBI endonuclease. The progress of each reaction was monitored by measuring the fluorescence intensity of a DNA intercalating dye. Values represent the fluorescence mean  $\pm$  standard deviation of triplicate reactions.

The biological function of isomiRs can vary with the number of nucleotides in the 5' region. This region can also modulate SNAP reconfiguration into the asymmetric DNA hairpin loop that activates the DNA circuit (Scheme 1A, III). Therefore, the impact of changing the number of nucleotides incorporated in the 3' region of the SNAP during reverse transcription was monitored in real time.

Including all 4 nucleotide triphosphates in the reverse transcription reaction enabled 7 nucleotides to be incorporated at the 3' end of the SNAP. This promoted formation of a stable asymmetric DNA hairpin that initiated rapid DNA amplification as expected (Figure 6A). Omitting adenosine during reverse transcription generated an asymmetric hairpin loop with a single 3' nucleotide truncation. This did not appear to influence the stability of the asymmetric hairpin loop since it also resulted in rapid DNA amplification (Figure 6B). Omitting thymine and adenine prematurely terminated reverse transcription to generate an 'activated' probe truncated by 5 nucleotides. Despite the 5 nucleotide truncation, a minor increase in fluorescence was detected (Figure 6C), however, the rate of amplification was reduced 12 fold during the early stages of the reaction. This was attributed to the reduced thermal stability of

the resultant DNA hairpin (Scheme 1A, III), which was further reduced when only guanine was added to the reverse transcription reaction to generate an 'activated' probe truncated by 6 nucleotides (Figure 6D).

This strategy of omitting a specific nucleotide to prematurely terminate reverse transcription can be used to precisely define the number of nucleotides incorporated into the probe so in principal, any region of a RNA transcript can be amplified to detectable levels using a carefully designed SNAP.

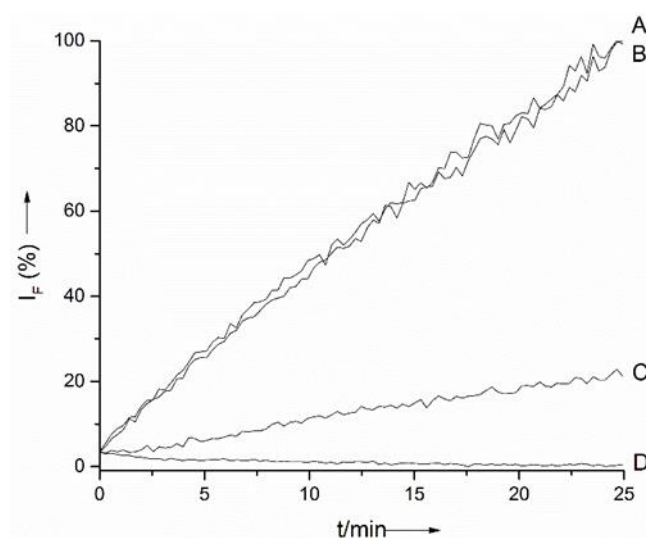


**Figure 6.** Fidelity of the activation switch: Replicate reverse transcription reactions containing 2.8 pmole of the synthetic miRNA were prepared, each containing different nucleotide triphosphates: A) contained dGTP, dCTP, dTTP and dATP to generate an 'activated' probe containing 7 nucleotides in the 3' region, B) contained dGTP, dCTP and dTTP to generate an 'activated' probe with a single 3' nucleotide truncation, C) contained dGTP and dCTP to generate an 'activated' probe truncated by 5 nucleotides and D) contained dGTP to generate an 'activated' probe truncated by 6 nucleotides. Residual RNA was hydrolysed and the 'activated' SNAPs were amplified using Bst DNA polymerase and Nt.BstNBI endonuclease. The progress of each amplification reaction was monitored in real time by measuring the fluorescence intensity.

The biological circuit maintains a high level of selective activation in a complex nucleic acid extract. A time course of detection, amplification and signal transduction initiated with different amounts of a synthetic miRNA in a heterogeneous RNA extract is demonstrated in Figure 7. Within minutes there was a noticeable increase in fluorescent signal emitted from reactions that contained a large amount of the miRNA (Figure 7A). When the reaction was initiated with 1.72 pmol of miRNA there was a 20 fold increase in fluorescent signal within 2.7 min, which increased beyond 100 fold within 25 min. The fluorescent signal emitted from the reaction decreased as the amount of miRNA was reduced indicating the circuit can be used to measure changes in the level of a specific miRNA (Figure 7B, C & D). When the amount decreased below 85.9 fmol no detectable increase in fluorescence was observed after the reaction had

progressed for 25 min (Figure 7E). In its current form, this is the activation threshold of the circuit, which represents  $5.2 \times 10^{10}$  copies (8.6 nM) of miRNA. This detection limit may be subject to improvement since the threshold for signal amplification of a synthetic 'asymmetric DNA hairpin' (Scheme 1A, III) was found to be  $3.4 \times 10^8$  copies (0.57 fmol) (Supplementary Figure S6). It is clear the SNAP maintains a high level of selectivity since no amplification and signal transduction was detected when the miRNA was omitted from the reaction, despite the presence of heterogeneous RNA (Figure 7E).

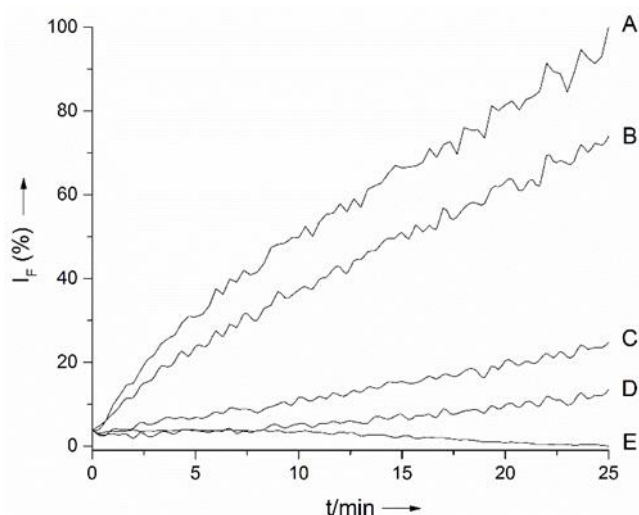


**Figure 7.** Qualitative detection: Replicate reactions containing the probe, 600 ng of heterogeneous RNA and reverse transcriptase were prepared and a different concentration of synthetic miRNA was added to each vessel (A: 1718 fmol, B: 859 fmol, C: 171 fmol, D: 85.9 fmol and E: no miRNA). Residual RNA was hydrolysed and the 'activated' DNA products were amplified using Bst large fragment DNA polymerase and Nt.BstNBI endonuclease. The progress of each reaction was monitored by measuring the fluorescence intensity

## Conclusions

In summary, a DNA circuit has been devised that enables qualitative detection of a specific miRNA. The simple and flexible biological circuit is composed of a series of integrated molecular switches designed to selectively detect and amplify miRNA to a level suitable for signal transduction. This is achieved using a carefully designed DNA probe that is 'activated' by a specific miRNA during a reverse transcription reaction. A small amount of the "activated" probe is then isothermally amplified to detectable levels using DNA polymerase and a nicking endonuclease in a subsequent enzymatic reaction. We have demonstrated that probes can be designed to detect sequence variations in 5' isomiRs and although single nucleotide truncations in the 5' region of a miRNA were undetectable in the current format, larger decreases in the number of nucleotides in the 5' region of a miRNA could be identified. In principal, the

circuit could also be tailored to detect any desired RNA transcript with a high level of specificity and sensitivity, by omitting nucleotides during reverse transcription to modulate SNAP reconfiguration and amplification. Trace amounts (85.9 fmol, 8.6nM) of a miRNA transcript in a purified heterogeneous RNA extract, can be rapidly amplified to detectable levels in real time under isothermal conditions. This strategy also has the potential to detect isomiRs in crude analytes by performing reverse transcription in cell lysates [16]. Since a small amount (1  $\mu$ L) is required for amplification in a subsequent reaction, inhibitors will be substantially diluted, which may obviate the need for miRNA purification and further simplify isomiR analysis.

## Experimental Section

The oligonucleotide probes (Geneworks) and the synthetic RNA target (Sigma) listed in Table 1, were dissolved in 18  $\Omega$ . cm Milli-Q water. Heterogeneous RNA was extracted from HEK 293 cells using TRIZOL (Invitrogen), as outlined by the manufacturer. The RNA was precipitated with the addition of 3M sodium acetate and ethanol and the purity and concentration of the nucleic acids was determined by measuring the optical density at 260 nm and 280 nm.

**SNAP amplification:** The synthetic miRNA was reverse transcribed in a 10  $\mu$ L reaction containing 800 nM Probe, 50 mM tris-HCl, 75 mM KCl, 3 mM  $MgCl_2$ , 10 mM dithiothreitol, and 250 nM dNTPs at pH 8.3. The mixture was heated to 70  $^{\circ}C$  for 10 min and cooled on ice before the addition of 200 U of M-MuLV reverse transcriptase (New England Biolabs). The reaction was incubated for 1 h at 37  $^{\circ}C$  then the enzyme was thermally denatured for 5 min at 95  $^{\circ}C$ . Excess RNA was digested by incubating the reaction with 2.5 U of RNase H and 25 U of RNase If (New England Biolabs) for 60 min at 37  $^{\circ}C$ .

The amplification reaction contained 100 mM NaCl, 50 mM tris-HCl, 10 mM  $MgCl_2$ , 1 mM dithiothreitol, pH 7.9, 125 nM dNTPs, 0.05% Triton X100, 5  $\mu$ M Syto 9, 0.27 U Bst large fragment DNA polymerase and 0.33 U Nt.BstNBI nicking endonuclease (New England Biolabs). Reactions were assembled at 4  $^{\circ}C$  and initiated by adding 1  $\mu$ L of reverse transcribed miRNA. The mixture was incubated at 55  $^{\circ}C$  in a real time PCR machine (Corbett Rotogene) and fluorescent measurements were made at 17 s intervals using an excitation wavelength of 470 nm and a detection wavelength of 510 nm. Syto 9 fluorescence was normalised to an internal reference (Cy5) present in an equal amount in each reaction. Values represent the percentage of Syto 9 fluorescence in each reaction.

Reaction products were analysed using 20% w/v TBE polyacrylamide gels (Invitrogen) run at 50 V. Gels were stained with ethidium bromide and visualised with UV illumination.

## Acknowledgements

We gratefully acknowledge support and funding from the National Breast Cancer Foundation (NBCF), Cancer Australia and the Australian Research Council: Future Fellowship Grant No. FT130100211.

**Keywords:** miRNA detection • Molecular Circuit • DNA nanotechnology • isothermal amplification

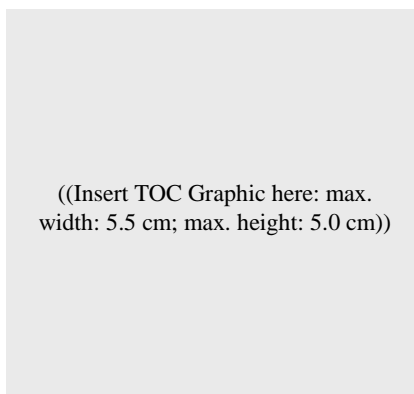
- [1] a) Y. Okada, T. Muramatsu, N. Suita, M. Kanai, E. Kawakami, V. Iotchkova, N. Soranzo, J. Inazawa, T. Tanaka, *Sci Rep* **2016**, *6*, 22223; b) M. Sandquist, H. R. Wong, *Expert Rev Clin Immunol* **2014**, *10*, 1349-1356; c) F. J. Slack, J. B. Weidhaas, *N Engl J Med* **2008**, *359*, 2720-2722.
- [2] P. Landgraf, M. Rusu, R. Sheridan, A. Sewer, N. Iovino, A. Aravin, S. Pfeffer, A. Rice, A. O. Kamphorst, M. Landthaler, C. Lin, N. D. Socci, L. Hermida, V. Fulci, S. Chiaretti, R. Foa, J. Schliwka, U. Fuchs, A. Novosel, R. U. Muller, B. Schermer, U. Bissels, J. Inman, Q. Phan, M. Chien, D. B. Weir, R. Choksi, G. De Vita, D. Frezzetti, H. I. Trompeter, V. Hornung, G. Teng, G. Hartmann, M. Palkovits, R. Di Lauro, P. Wernet, G. Macino, C. E. Rogler, J. W. Nagle, J. Ju, F. N. Papavasiliou, T. Benzinger, P. Lichter, W. Tam, M. J. Brownstein, A. Bosio, A. Borkhardt, J. J. Russo, C. Sander, M. Zavolan, T. Tuschl, *Cell* **2007**, *129*, 1401-1414.
- [3] T. A. Farazi, J. I. Hoell, P. Morozov, T. Tuschl, *Adv Exp Med Biol* **2013**, *774*, 1-20.
- [4] a) C. Chen, D. A. Ridzon, A. J. Broomer, Z. Zhou, D. H. Lee, J. T. Nguyen, M. Barbisin, N. L. Xu, V. R. Mahuvakar, M. R. Andersen, K. Q. Lao, K. J. Livak, K. J. Guegler, *Nucleic Acids Res* **2005**, *33*, e179; b) T. D. Schmittgen, J. Jiang, Q. Liu, L. Yang, *Nucleic Acids Res* **2004**, *32*, e43; c) T. D. Schmittgen, E. J. Lee, J. Jiang, A. Sarkar, L. Yang, T. S. Elton, *Chen, Methods* **2008**, *44*, 31-38; d) R. Shi, V. L. Chiang, *Biotechniques* **2005**, *39*, 519-525; e) X. Xie, F. Tang, Z. Yang, Y. Zhang, Z. Feng, Y. Yang, X. Wu, F. Zhang, J. Zhu, K. Xu, *Sci Rep* **2015**, *5*, 9356.
- [5] Y. Zhao, F. Chen, Q. Li, L. Wang, C. Fan, *Chem Rev* **2015**, *115*, 12491-12545.
- [6] a) N. E. Larkey, C. K. Almie, V. Tran, M. Egan, S. M. Burrows, *Anal Chem* **2014**, *86*, 1853-1863; b) F. Li, J. Peng, J. Wang, H. Tang, L. Tan, Q. Xie, S. Yao, *Biosens Bioelectron* **2014**, *54*, 158-164; c) U. H. Yildiz, P. Alagappan, B. Liedberg, *Anal Chem* **2013**, *85*, 820-824.
- [7] a) K. Hosoda, T. Matsuura, H. Kita, N. Ichihashi, K. Tsukada, I. Urabe, T. Yomo, *Rna-a Publication of the RNA Society* **2008**, *14*, 584-592; b) S. P. Jonstrup, J. Koch, J. Kjems, *RNA* **2006**, *12*, 1747-1752; c) A. Ogawa, *Bioorg Med Chem Lett* **2010**, *20*, 6056-6060; d) X. P. Wang, B. C. Yin, P. Wang, B. C. Ye, *Biosens Bioelectron* **2013**, *42*, 131-135; e) Y. Q. Wen, Y. Xu, X. H. Mao, Y. L. Wei, H. Y. Song, N. Chen, Q. Huang, C. H. Fan, D. Li, *Anal Chem* **2012**, *84*, 7664-7669; f) B. C. Yin, Y. Q. Liu, B. C. Ye, *Anal Chem* **2013**, *85*, 11487-11493; g) B. Yoo, A. Kavishwar, S. K. Ghosh, N. Barteneva, M. V. Yigit, A. Moore, Z. Medarova, *Chem Biol* **2014**, *21*, 199-204.
- [8] Y. Shen, F. Tian, Z. Chen, R. Li, Q. Ge, Z. Lu, *Biosens Bioelectron* **2015**, *71*, 322-331.
- [9] F. J. Slack, *Clin Chem* **2013**, *59*, 325-326.
- [10] a) F. Wang, X. Liu, I. Willner, *Angew Chem Int Ed Engl* **2015**, *54*, 1098-1129; b) A. R. Connolly, M. Trau, *Angew Chem Int Ed Engl* **2010**, *49*, 2720-2723; c) W. U. Dittmer, F. C. Simmel, *Nano Letters* **2004**, *4*, 689-691; d) C. Mao, W. Sun, Z. Shen, N. C. Seeman, *Nature* **1999**, *397*, 144-146; e) S. Modi, M. G. Swetha, D. Goswami, G. D. Gupta, S. Mayor, Y. Krishnan, *Nature Nanotechnology* **2009**, *4*, 325-330; f) S. Venkataraman, R. M. Dirks, P. W. Rothmund, E. Winfree, N. A. Pierce, *Nat Nanotechnol* **2007**, *2*, 490-494; g) Y. Weizmann, M. K. Beissenhirtz, Z. Cheglakov, R. Nowarski, M. Kotler, I. Willner, *Angew Chem Int Ed Engl* **2006**, *45*, 7384-7388.
- [11] a) A. R. Connolly, M. Trau, *Nat Protoc* **2011**, *6*, 772-778; b) W. J. Gao, X. Li, L. W. Zeng, T. Peng, *Diagnostic Microbiology and Infectious Disease* **2008**, *60*, 133-141; c) G. T. Walker, M. C. Little, J. G. Nadeau, D. D. Shank, *Proc Natl Acad Sci U S A* **1992**, *89*, 392-396; d) N. G. Walter, G. Strunk, *Proc Natl Acad Sci U S A* **1994**, *91*, 7937-7941; e) Q. Zhang, F. Chen, F. Xu, Y. Zhao, C. Fan, *Anal Chem* **2014**, *86*, 8098-8105.
- [12] J. J. DeStefano, R. G. Buiser, L. M. Mallaber, T. W. Myers, R. A. Bambara, P. J. Fay, *J Biol Chem* **1991**, *266*, 7423-7431.
- [13] C. T. Neilsen, G. J. Goodall, C. P. Bracken, *Trends Genet* **2012**, *28*, 544-549.
- [14] a) P. Mestdagh, N. Hartmann, L. Baeriswyl, D. Andreasen, N. Bernard, C. Chen, D. Cheo, P. D'Andrade, M. DeMayo, L. Dennis, S. Derveaux, Y. Feng, S. Fulmer-Smentek, B. Gerstmayer, J. Gouffon, C. Grimley, E. Lader, K. Y. Lee, S. Luo, P. Mouritzen, A. Narayanan, S. Patel, S. Peiffer, S. Ruberg, G. Schroth, D. Schuster, J. M. Shaffer, E. J. Shelton, S. Silveria, U. Ulmanella, V. Veeramachaneni, F. Staedtler, T. Peters, T. Guettouche, L. Wong, J. Vandesompele, *Nat Methods* **2014**, *11*, 809-815; b) N. Redshaw, T. Wilkes, A. Whale, S. Cowen, J. Huggett, C. A. Foy, *Biotechniques* **2013**, *54*, 155-164.
- [15] a) J. D. Roberts, K. Bebenek, T. A. Kunkel, *Science* **1988**, *242*, 1171-1173; b) J. Stenesh, P. K. Gupta, *Biochem Biophys Res Commun* **1981**, *101*, 230-236; c) A. Varela-Echavarría, N. Garvey, B. D. Preston, J. P. Dougherty, *J Biol Chem* **1992**, *267*, 24681-24688.
- [16] G. Van Peer, P. Mestdagh, J. Vandesompele, *Sci Rep* **2012**, *2*, 222.

**Entry for the Table of Contents** (Please choose one layout)

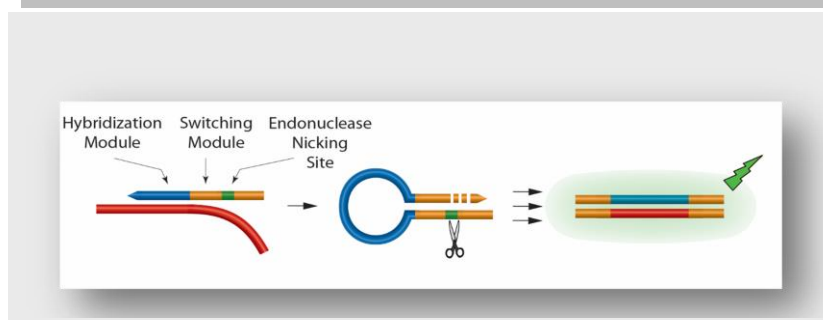
Layout 1:

**FULL PAPER**

Text for Table of Contents

*Author(s), Corresponding Author(s)\****Page No. – Page No.****Title**

Layout 2:

**FULL PAPER***Ashley R. Connolly#\*, Rena Hirani‡, Amanda V Ellis# and Matt Traut\*†***Page No. – Page No.****A DNA Circuit for IsomiR Detection**